ACS Macro Letters

Letter

pubs.acs.org/macroletters

Self-Assembly of Monodisperse versus Bidisperse Polymer-Grafted Nanoparticles

Dan Zhao,[†] Matteo Di Nicola,[‡] Mohammad M. Khani,[§] Jacques Jestin,[†,∥] Brian C. Benicewicz,[§] and Sanat K. Kumar*[,†]

[†]Department of Chemical Engineering, Columbia University, 500 West 120th Street, New York, New York 10027, United States

[‡]School of Science and Technology, Università di Camerino, Via Sant'Agostino 1, 62032, Camerino, Italy

[§]Department of Chemistry and Biochemistry, University of South Carolina, Columbia, South Carolina 29208, United States

[∥]Laboratoire Léon Brillouin, CEA Saclay, 91191 Gif-sur-Yvette Cedex, France

Supporting Information

ABSTRACT: We systematically compare the dispersion and self-assembly of silica nanoparticles (NPs) grafted with either a sparse monomodal long chain length polystyrene (PS) brush or a bimodal brush comprised of a sparse grafting of long PS chains and a dense carpet of short poly(2-vinylpyridine) (P2VP) chains. These two different types of NPs are placed in pure PS matrices of varying molecular weights in a series of experiments. We first show that NP dispersion is generally improved in the case of bimodal brushes. More interestingly, at low PS grafting densities the bimodal brushes give different self-assembled structures relative to the monomodal brushes; we conjecture that the presence of the short P2VP chains in the bimodal brush reduces the effective core−core attractions and thus allows these bidisperse NPs to display self-assembly behavior that is less likely to be kinetically trapped by the strong intercore attractions that control the behavior of monomodal NPs. In this low PS grafting density limit, where we expect the spatial coverage of the brush to be the most nonuniform, we find the formation of "vesicular" structures that are representative of highly asymmetric ("tadpole") surfactants. Our results therefore show that reducing the inter-NP attractions gives rise to a much richer ensemble of NP self-assemblies, apparently with a smaller influence from kinetic traps (or barriers).

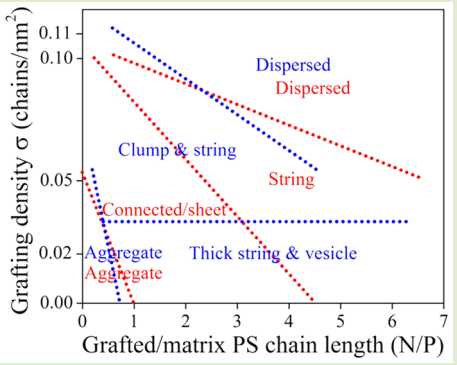

Polymer nanocomposites (PNCs), mixtures of nanometer-sized particles and polymer matrices, have attracted continuing interest over the past few decades, primarily because they offer the promise of significant property improvements relative to the pure polymer.[1−6] The mixing of inorganic nanoparticles (NP) with typically hydrophobic polymers, however, is challenging because of their strong energetic dislike for each other. One common strategy to improve their miscibility is to covalently graft the NP surface with polymer chains possessing the same chemistry as the matrix.[7−9] Initially, monomodal[10−12] brushes were used to control particle/polymer miscibility. Interestingly, in these systems, anisotropic NP morphologies (strings, sheets, or connected structures) were observed when the NPs were sparsely grafted with polymer chains.[11,13,14] This finding was reconciled by the fact that lightly grafted NPs act akin to surfactants, that is, some parts of the particle surface are covered by the grafted chains ("hydrophobic"), while the other hydrophilic parts are exposed to the matrix.[15,16] Very recently bimodal brushes, consisting of a densely grafted, short brush (enthalpic screening for core−core attraction) and a sparsely grafted, long brush (favorable entropic interactions with the matrix chains) have been studied as a route to further improve NP dispersion.[17−21] Again, all the chains were of the same chemistry. These bimodal polymer grafted NPs were found to be well-dispersed across a broad range of matrix molecular weights, a fact that is attributed to the significant reduction in attraction between the particles due to the presence of the short chain brush.[22] In a slightly different vein, Ferrier et al.[23] reported that the dispersion states of gold nanorods grafted with bidisperse mixed polymer brushes are markedly improved relative to those coated by monodisperse grafts or bidisperse grafts with the same chemistry. While this bimodal brush idea is therefore an effective, well-appreciated strategy for improving NP dispersion, there remain unresolved questions: (i) Does the anisotropic NP self-assembly seen for monomodal brushes still occur in the bimodal grafted system? This is interesting because these anisotropic superstructures help to optimize the mechanical properties of the polymer melts.[11] (ii) Is this bimodal idea general, that is, do mixed bimodal brushes also help improve the dispersion of spherical NPs when the long, sparse brush is chemically identical with the matrix, while the other short, dense one energetically

Received: May 5, 2016
Accepted: June 13, 2016
Published: June 16, 2016

© 2016 American Chemical Society

DOI: 10.1021/acsmacrolett.6b00349
ACS Macro Lett. 2016, 5, 790−795

Table 1. Grafting Characteristics of Mixed Bimodal PS-P2VP Grafted Silica NPs

P2VP brush			PS brush			
M_n (kg mol^{-1})	$Đ$	σ_{P2VP} (chains/nm^2)	M_n (kg mol^{-1})	$Đ$	σ_{PS} (chains/nm^2)	nomenclature
7	1.14	0.18	155	1.4	0.11	BM-0.11-155
6	1.09	0.18	157	1.4	0.05	BM-0.05-157
7.5	1.15	0.18	104	1.4	0.02	BM-0.02-104

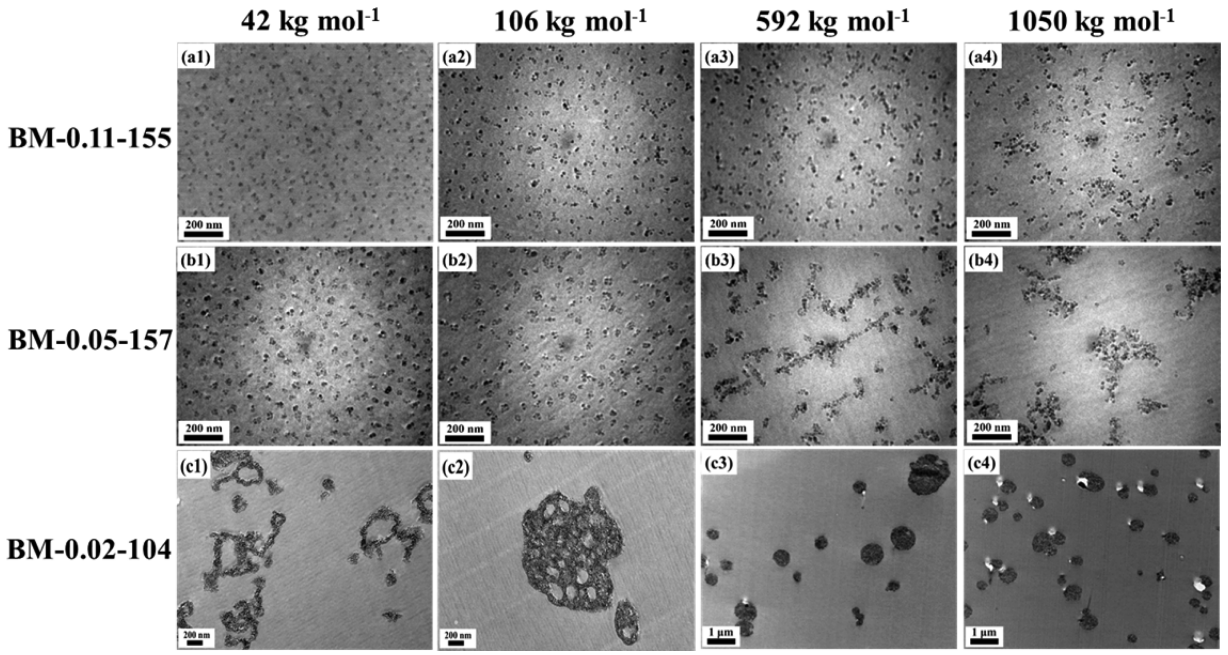

Figure 1. TEM micrographs for bimodal PS-P2VP grafted silica NPs in PS matrices of varying molecular weights. The grafting characteristics and matrix molecular weights are indicated inside the graph. Note that the scale bar is shown inside each micrograph. All nanocomposites contain 5 wt % in silica core. For representative TEM images of BM-0.02-104 particles in PS matrices of other molecular weights, please refer to Figure S4 in Supporting Information.

dislikes the matrix? We address both of these questions in this contribution. In particular, we have synthesized mixed bimodal polystyrene-poly(2-vinylpyridine) (PS-P2VP) brush coated silica NPs and investigated their dispersion behavior in PS matrices. By comparing the results of the monomodal and bimodal PS grafted NPs, we give insights into these questions.

Sample preparation: We synthesized three mixed bimodal PS-P2VP (sparse grafting of long PS chains and a short dense carpet of P2VP chains) grafted silica (with a core diameter of 14 ± 4 nm) NPs,[18] with the grafting characteristics (chain length M_n and dispersity $Đ$) presented in Table 1. Note that for the synthesis of these particles we have adopted a two-step "grafting from" strategy; thus, we expect the P2VP and PS brushes to be randomly mixed on the silica surface instead of being phase-separated into discrete domains. There, however, is no currently available experimental technique that allows us to characterize this mixing. We then studied their dispersion behavior in PS matrices of varying molecular weights (M_w = 17.7, 42, 65, 106, 592, and 1050 kg mol^{-1}, with $Đ$ = 1.04, 1.05, 1.03, 1.06, 1.09, and 1.08, respectively). The PNC samples were prepared by solvent casting from tetrahydrofuran (THF), followed by thermal annealing for 5 days at 150 °C under vacuum. For a detailed protocol of sample preparation and processing, please refer to Supporting Information. In this paper we shall first discuss the dispersion states of the mixed bimodal PS-P2VP coated silica particles in PS matrices and then compare their phase behavior with that of the monomodal PS and bimodal PS-PS analogs in common PS matrices.

Particle dispersion in solution: Before investigating the spatial organization of bimodal PS-P2VP grafted silica NPs in PS matrices, we first need to ensure that they are individually dispersed in THF solution. To that end, we performed small angle neutron and X-ray scattering experiments on suspensions of these particles in THF (0.1 wt % in silica core); since the primary contrast is between the silica core and the grafts/solvent, we are primarily sensitive to the core size and spatial dispersion of the NPs. We find that the scattering curves are well represented by a polydisperse sphere form factor with a radius of ∼7 nm and a log-normal dispersity of 0.25−0.3 (Figure S1 and Table S1 in Supporting Information). This is consistent with the value measured by TEM (∼7 ± 2 nm in radius) and manufacturer specifications (10−15 nm in diameter), indicating homogeneous dispersion of silica NPs.

Dispersion of bimodal PS-P2VP grafted NPs in polymer matrices: Figure 1 presents TEM images of nanocomposites loaded with bimodal PS-P2VP brush coated silica NPs with varying graft densities of the long PS chains in PS matrices of different molecular weights. We first show that, as expected, the dispersion of NPs is greatly improved with an increase in the PS grafting density (σ_{PS}). For instance, in a 42 kg mol^{-1} PS matrix (first column in Figure 1), we observe thick strings mixed with vesicle-like structures at a low grafting density (σ_{PS} = 0.02 chains/nm^2 or ∼12 chains per particle; Figure 1c1); at σ_{PS} =

DOI: 10.1021/acsmacrolett.6b00349
ACS Macro Lett. 2016, 5, 790−795

0.05 chains/nm^2 (or ∼31 chains per particle), small aggregates consisting of 3−6 primary particles form (Figure 1b1), while at σ_{PS} = 0.11 chains/nm^2 (or ∼68 chains per particle), the silica NPs are nearly individually dispersed (Figure 1a1). Note that similar trends in NP dispersion were also found in the other PS matrices (second to fourth columns in Figure 1). To quantify the change in NP dispersion as a function of PS grafting density, we also digitized the TEM images, appropriately thresholded them, and then calculated their pixel−pixel autocorrelation function, $C(r)$ (Figure S2 in Supporting Information). This image analysis shows that, as σ_{PS} decreases, the deviation from the initial slope in $C(r)$ occurs at a shorter distance, indicating increased NP clustering. In general, our findings can be attributed to the fact that, as the grafting density increases, the effective PS surface coverage of the NP surface increases. Thus, core−core attraction is increasingly screened and improved miscibility results. Here we note that the BM-0.02-104 has shorter PS brushes than the other two particles. Previous work has shown that equivalent behavior results across silica NPs with different grafting densities and chain lengths so long as we examine trends as a function of $\sigma_{PS}\sqrt{N}$ (where N is the grafted chain length).[4] The lower molecular weight of the PS brush in the last bimodal particle, relative to the other two NPs, could possibly enhance the degree of NP aggregation but should not yield new physics.

We have also examined the effect of matrix chain length on the spatial distribution of NPs. As shown in Figure 1 (first row), at σ_{PS} = 0.11 chains/nm^2, the NPs show increasing clustering with increases in the matrix PS molecular weight. This structural evolution as a function of matrix chain length is more pronounced at σ_{PS} = 0.05 chains/nm^2 (second row in Figure 1). In this case, small clusters (or clumps) form in low molecular weight matrices (Figure 1b1,b2); strings appear at intermediate chain length (Figure 1b3), and micron-sized agglomerates are observed for even longer matrix chains (Figure 1b4). These trends in NP dispersion versus matrix chain length are supported by $C(r)$ calculations (Figure S3 in Supporting Information). As shown there, in matrices with smaller molecular weights (42 and 106 kg mol^{-1}), we see a depletion "hole" at short distances, indicating repulsion between the particles or small clumps of the particles. In contrast, in higher molecular weight matrices (592 and 1050 kg mol^{-1}), $C(r)$ is essentially positive for all distances covered, indicating increased agglomeration. These findings are entropically driven, that is, as a result of the autophobic dewetting of the matrix from the brush. Inspired by arguments presented in the case of planar brushes, we suggest that when $\sigma_{PS}\sqrt{N} < (N/P)^2$ (where P is the matrix chain length), the favorable entropy resulting from mixing the matrix with the long PS brush leads to an effective repulsion between the particles, as indicated by a correlation hole in $C(r)$. In the opposite case, where $\sigma_{PS}\sqrt{N} > (N/P)^2$, particles are attracted to each other as the brush chains are not soluble in the matrices. In this same spirit, at σ_{PS} = 0.02 chains/nm^2, the NP assemblies evolve from thick strings and vesicles in a 42 kg mol^{-1} matrix (Figure 1c1) to large spherical aggregates at higher molecular weights (Figure 1c3,c4).

Going further, two more interesting things are noted from Figure 1. First, we see a variety of new structures formed by these bimodal grafted NPs. For example, strings form when bimodal brush coated silica NPs (BM-0.05-157) are placed in a 592 kg mol^{-1} PS matrix (Figure 1b3); thick strings and vesicles form when BM-0.02-104 is placed in 42 or 65 kg mol^{-1} PS (Figure 1c1 and Figure S4 in Supporting Information); clumps form when BM-0.05-157 is placed in 42 or 106 kg mol^{-1} PS matrices (Figure 1b1,b2). These results are new since previous work on bimodal grafted NPs found only particle dispersion or macrophase separation (see below for more on this topic).[17,19] In the previous work, the short brush, the long brush, and the matrix were chemically identical. The short brush therefore serves to (strongly) reduce the effective core−core attraction. In our case, as in this previous work, the P2VP brush also mediates core−core attractions by increasing the minimum approach distance of the NPs.[24] However, as we shall show below (Figure 4), the repulsion between the P2VP chains and the PS matrix serves to increase the effective intercore attractions, but not as much as to be comparable to the bare silica case. These relatively stronger attractions yield these new self-assembled structures.[25] Another interesting point is that the large agglomerates formed by BM-0.05-157 particles in a 1050 kg mol^{-1} matrix have more open, loosely packed morphologies compared to the ones consisting of BM-0.02-104 particles (Figure 1b4 vs c4). This is presumably a consequence of the balance between the enthalpy gain from core−core contacts and the entropy loss due to deformation of the long PS brushes. In other words, at σ_{PS} = 0.05 chains/nm^2, the number of grafted PS chains is still large enough to create an energy barrier for particles to collapse into a compact cluster. In contrast, at σ_{PS} = 0.02 chains/nm^2, the core−core interaction dominates so that the small numbers of PS brush chains can be more readily squeezed into the interparticle spaces. Alternatively, other factors associated with nonuniformity of the grafting process might play a role. One possibility is the fluctuation in the number of PS brush chains among various silica NPs (especially at σ_{PS} = 0.02 chains/nm^2), as discussed by Hakem et al.[26] A second possibility is the anisotropic coverage of the NP by the grafted chains, an effect that causes these NPs to act akin to Janus particles.[15]

Self-assembly of monodisperse versus bidisperse grafted NPs: Based on the TEM micrographs shown in Figure 1, we construct a morphology diagram for bimodal PS-P2VP silica NPs in PS matrices (Figure 2). Depending on the grafting density of the PS brush and the grafted/matrix PS chain length ratio (N/P), the NP structures formed in the PS matrices are classified as dispersed, clump & string, thick string & vesicle,

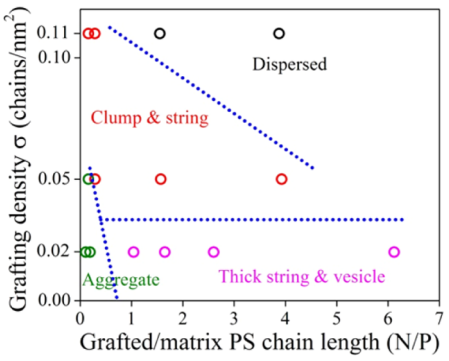

Figure 2. Experimental morphology diagram of bimodal PS-P2VP tethered silica NPs mixed with PS matrices. The black, red, pink, and green circles correspond to "Dispersed", "Clump & string", "Thick string & vesicle", and "Aggregate", respectively. The blue dotted lines, indicating the structural boundaries, are guides to the eye. Note that most of the data points shown here are from Figure 1, with some others presented in Figure S4 in Supporting Information.

DOI: 10.1021/acsmacrolett.6b00349
ACS Macro Lett. 2016, 5, 790−795

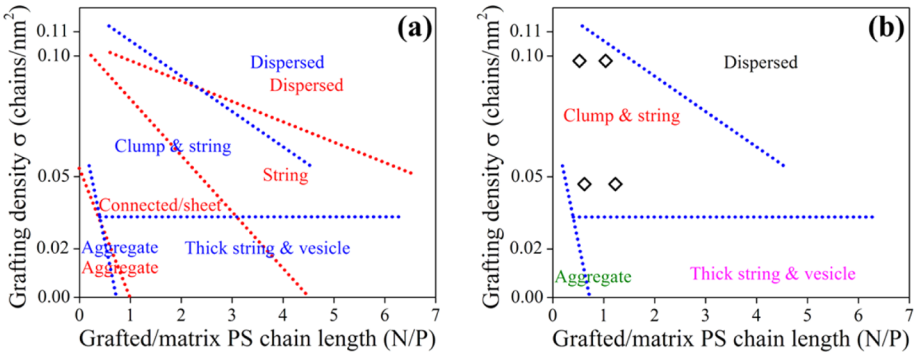

Figure 3. (a) Comparison of the dispersion morphology diagram of silica NPs coated by monomodal PS and bimodal PS-P2VP brushes in PS matrices. The blue dotted lines correspond to morphology boundaries in the bimodal system, that is, "Dispersed", "Clump & String", "Thick string & vesicle", and "Aggregate". The red dotted lines are for the monomodal PS grafted system from ref 11.: "Dispersed", "String", "Connected/sheet", and "Aggregate". (b) Plot of the NP structures of the bimodal PS-PS coated silica NPs in PS matrices (the black diamonds, all well dispersed) from ref 19 in the bimodal morphology diagram constructed in Figure 2.

and aggregates. We compare this self-assembly behavior to NPs grafted with monomodal PS (II) (Figure 3a).

First, the regions for the extreme cases of well dispersed NPs ("Dispersed") and complete phase separation ("Aggregate") are similar between these two systems. However, our previous work has suggested that the sheet-like structure observed for monomodal brushes in fact corresponds to a directionally phase separated state.[27] In contrast, the BM-0.05-157 NPs self-assemble into strings in a 592 kg mol^{-1} PS matrix (the corresponding monomodal analog forms connected sheets or phase separated state, Figure 3a). This immediately suggests that the dense P2VP carpet reduces the effective core−core attraction, making NPs generally more miscible (dispersed) compared to the monomodal PS brush case. A straightforward calculation suggests that the London dispersion forces ("Hamaker interactions") between a pair of NP cores reduces from $\sim 5k_BT$ (monomodal) to $\sim 0.4k_BT$ (bimodal) at an interparticle separation of 0.1 nm (Figure 4). These results suggest that, even though anisotropic NP superstructures can still form from the bimodal mixed brush coated particles, apparently the reduced attraction strength between silica cores reduces the region in parameter space where these structures form. This "suppression" of the regime where self-assembled structures form was previously anticipated by the theoretical work of Pryamtisyn et al.[25]

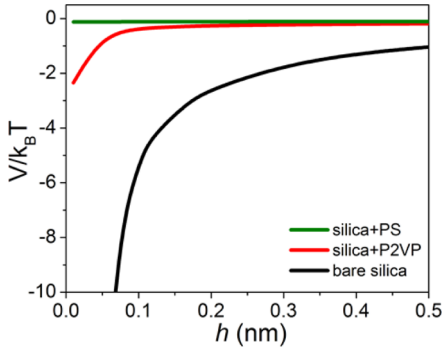

Figure 4. Interparticle core−core London dispersion potential (V/k_BT) as a function of separation (h) between the outer layers of the particles. The black curve is that between bare silica NPs, the red and green curves correspond to silica NPs coated with a surface layer of P2VP and PS, respectively. Note that the surface layer for both P2VP and PS comprises 7 kg mol^{-1} chains with a grafting density of 0.18 chains/nm^2, yielding shell thicknesses of 1.54 and 2.09 nm, respectively (see Supporting Information for details).

Next we compare the dispersion behavior of bimodal PS-P2VP (I) tethered silica NPs and bimodal long PS-short, densely grafted PS (III) tethered silica NPs in PS matrices. As shown in Figure 3b (also see Figure 1b1,b2), we observe clumps when the BM-0.05-157 (PS-P2VP) particles are placed in a 42 or 106 kg mol^{-1} PS matrix, while bimodal PS-PS particles with similar grafting characteristics (for short PS brush, M_n = 7.2 kg mol^{-1}, σ_{PS} = 0.18 chains/nm^2; for long PS brush, M_n = 118 kg mol^{-1}, σ_{PS} = 0.047 chains/nm^2 from ref 19) are well dispersed in PS matrices of 190 kg mol^{-1}.[19] This result can be reconciled by the much weaker core−core attractions in (III) as compared to (I), as shown in Figure 4. Interestingly, very recently, Ferrier et al.[23] have shown that gold nanorods grafted with mixed, bidisperse polymer brushes are much better dispersed than their bidisperse homopolymer analogs in the same polymer matrices. This previous work used the high grafting density regime for both brushes (>0.24 chains/nm^2), where the inner brush should be completely shielded by the outer grafts. Also, as the chain length of the two brushes are comparable, this work suggests that the short grafted chains force the longer ones to be more stretched and thus promote miscibility with the matrix chains. In contrast, in our system, as the PS grafting density is significantly smaller and its chain length is much longer than P2VP, the core−core attraction still plays an important role and we would expect negligible change in the conformation of PS chains. Therefore, we believe that different mechanisms control NP dispersion behavior in these two limits of high and low grafting density, respectively.

Finally, we focus on the formation of the interesting structures (thick strings and vesicles) when placing BM-0.02-104 particles into a 42 kg mol^{-1} PS matrix (Figure 1c1, also see Figure S4 where PS matrices of 17.7 or 65 kg mol^{-1} are used). The strings (open or closed) formed have a typical thickness of ~100 nm (~7−8 NPs wide). Apparently, the particle−particle attraction dominates even in such cases where the long PS brush (104 kg mol^{-1}) favorably interacts with the matrix chains. Also, we believe that this could be due to the inherent fluctuation in both the number of chains among various particles as well as the distribution of grafted chains on one single particle, especially in the limit of sparse grafting. In fact, recent simulation, theory and experiments suggest that, for small number of grafts, their spatial distribution on spherical NPs is anisotropic and asymmetric.[15,16,28] On the other hand,

DOI: 10.1021/acsmacrolett.6b00349
ACS Macro Lett. 2016, 5, 790−795

Hakem et al.[26] reported that, in the case of small number of functional sites per particle, the distribution in the number of ligands on various particles significantly broadens. Additionally, we also note that the polydisperse size of the silica core (Table S1 in Supporting Information) might also contribute to the polydispersity in the grafting density of different particles. These facts, in combination, allow us to conjecture that the particles with small number of grafted PS chains prefer to be placed in the interior of the thick strings or vesicles, while those with larger number of grafts can favorably interact with the PS matrix, thus, decorating the outside of the clusters. Moreover, we recall that these new structures are not observed in the monomodal system, even at lower grafting densities (e.g., 0.01 chains/nm^2, as shown in ref 11). Apparently, the formation of these more complicated structures require weaker effective attractions between NP cores, which allows the structures to reorganize more readily. In contrast, the monomodal PS coated particles have much stronger core−core attractions and thus are much more easily kinetically trapped once they touch each other. Interestingly, similar microscale string-like NP assemblies were previously observed in side chain fullerene polymers.[29] However, the underlying physics responsible for the formation of these interesting NP morphologies is still not clear. Current efforts (both experiments and simulations) are in progress to understand the general mechanisms responsible for these more complex self-assembly processes.

Conclusions: We have systematically examined the dispersion and assembly of bimodal PS-P2VP grafted silica NPs in PS matrices. We first show that, depending on the PS grafting density and the ratio of grafted/matrix chain length, the NP dispersion states in the PS matrices can be tuned from aggregate, thick string & vesicle, clump & string to dispersed phases. By comparing to the behavior of the monomodal PS-coated silica NPs, we then show that anisotropic NP self-assembly still occurs in the bimodal system. However, there is a general shift toward better-dispersed phases when the silica core−core attraction is reduced due to the presence of the dense P2VP layers around the NPs. However, due to the relatively stronger core−core attractions (especially at short distances), these mixed PS-P2VP brush tethered particles are less dispersed than NPs grafted with bimodal PS-PS brushes in PS matrices of comparable molecular weights. Finally, we observe vesicle-like NP structures for mixed bimodal brush grafted NPs of lower PS grafting density blended with short PS matrices. This finding is attributed to the weaker interparticle interactions, which lead to self-assembly behavior that is less kinetically trapped than their monomodal analogs. The relatively large thickness of the walls of these vesicular structures apparently results from the strong fluctuation in both the number of chains among various particles and the distribution of grafted chains on a NP's surface in the limit of sparse grafting.

■ ASSOCIATED CONTENT

Supporting Information

The Supporting Information is available free of charge on the ACS Publications website at DOI: 10.1021/acsmacrolett.6b00349.

Experimental details (PDF).

■ AUTHOR INFORMATION

Corresponding Author

*E-mail: sk2794@columbia.edu.

Notes

The authors declare no competing financial interest.

■ ACKNOWLEDGMENTS

The authors thank the National Science Foundation (DMR-1408323) for financial support of this work. NYULMC OCS Microscopy Core is also acknowledged for help with microtome and TEM.

■ REFERENCES

(1) Gilman, J. W. *Appl. Clay Sci.* **1999**, *15*, 31−49.
(2) Winey, K. I.; Kashiwagi, T.; Mu, M. *MRS Bull.* **2007**, *32*, 348−353.
(3) Choudalakis, G.; Gotsis, A. D. *Eur. Polym. J.* **2009**, *45*, 967−984.
(4) Kumar, S. K.; Jouault, N.; Benicewicz, B.; Neely, T. *Macromolecules* **2013**, *46*, 3199−3214.
(5) Hashemi, A.; Jouault, N.; Williams, G. A.; Zhao, D.; Cheng, K. J.; Kysar, J. W.; Guan, Z.; Kumar, S. K. *Nano Lett.* **2015**, *15*, 5465−5471.
(6) Zhao, D.; Ge, S.; Senses, E.; Akcora, P.; Jestin, J.; Kumar, S. K. *Macromolecules* **2015**, *48*, 5433−5438.
(7) Li, C.; Benicewicz, B. C. *Macromolecules* **2005**, *38*, 5929−5936.
(8) Li, C.; Han, J.; Ryu, C. Y.; Benicewicz, B. C. *Macromolecules* **2006**, *39*, 3175−3183.
(9) Barbey, R.; Lavanant, L.; Paripovic, D.; Schüwer, N.; Sugnaux, C.; Tugulu, S.; Klok, H.-A. *Chem. Rev.* **2009**, *109*, 5437−5527.
(10) Chevigny, C.; Dalmas, F.; Di Cola, E.; Gigmes, D.; Bertin, D.; Boué, F.; Jestin, J. *Macromolecules* **2011**, *44*, 122−133.
(11) Akcora, P.; Liu, H.; Kumar, S. K.; Moll, J.; Li, Y.; Benicewicz, B. C.; Schadler, L. S.; Acehan, D.; Panagiotopoulos, A. Z.; Pryamitsyn, V.; Ganesan, V.; Ilavsky, J.; Thiyagarajan, P.; Colby, R. H.; Douglas, J. F. *Nat. Mater.* **2009**, *8*, 354−359.
(12) Xu, C.; Ohno, K.; Ladmiral, V.; Composto, R. J. *Polymer* **2008**, *49*, 3568−3577.
(13) Maillard, D.; Kumar, S. K.; Rungta, A.; Benicewicz, B. C.; Prud'homme, R. E. *Nano Lett.* **2011**, *11*, 4569−4573.
(14) Green, P. F. *Soft Matter* **2011**, *7*, 7914−7926.
(15) Bozorgui, B.; Meng, D.; Kumar, S. K.; Chakravarty, C.; Cacciuto, A. *Nano Lett.* **2013**, *13*, 2732−2737.
(16) Asai, M.; Cacciuto, A.; Kumar, S. K. *Soft Matter* **2015**, *11*, 793−797.
(17) Li, Y.; Tao, P.; Viswanath, A.; Benicewicz, B. C.; Schadler, L. S. *Langmuir* **2013**, *29*, 1211−1220.
(18) Rungta, A.; Natarajan, B.; Neely, T.; Dukes, D.; Schadler, L. S.; Benicewicz, B. C. *Macromolecules* **2012**, *45*, 9303−9311.
(19) Natarajan, B.; Neely, T.; Rungta, A.; Benicewicz, B. C.; Schadler, L. S. *Macromolecules* **2013**, *46*, 4909−4918.
(20) Nair, N.; Wentzel, N.; Jayaraman, A. *J. Chem. Phys.* **2011**, *134*, 194906.
(21) Martin, T. B.; Jayaraman, A. *Macromolecules* **2013**, *46*, 9144−9150.
(22) Raghavan, S. R.; Hou, J.; Baker, G. L.; Khan, S. A. *Langmuir* **2000**, *16*, 1066−1077.
(23) Ferrier, R. C., Jr; Koski, J.; Riggleman, R. A.; Composto, R. J. *Macromolecules* **2016**, *49*, 1002.
(24) Jouault, N.; Lee, D.; Zhao, D.; Kumar, S. K. *Adv. Mater.* **2014**, *26*, 4031−4036.
(25) Pryamtisyn, V.; Ganesan, V.; Panagiotopoulos, A. Z.; Liu, H.; Kumar, S. K. *J. Chem. Phys.* **2009**, *131*, 221102.
(26) Hakem, I. F.; Leech, A. M.; Johnson, J. D.; Donahue, S. J.; Walker, J. P.; Bockstaller, M. R. *J. Am. Chem. Soc.* **2010**, *132*, 16593−16598.
(27) Akcora, P.; Kumar, S. K.; García Sakai, V.; Li, Y.; Benicewicz, B. C.; Schadler, L. S. *Macromolecules* **2010**, *43*, 8275−8281.

DOI: 10.1021/acsmacrolett.6b00349
ACS Macro Lett. 2016, 5, 790−795

(28) Koch, A. H.; Lévêque, G.; Harms, S.; Jaskiewicz, K.; Bernhardt, M.; Henkel, A.; Sönnichsen, C.; Landfester, K.; Fytas, G. *Nano Lett.* **2014**, *14*, 4138−4144.
(29) Li, J.; Benicewicz, B. C. *J. Polym. Sci., Part A: Polym. Chem.* **2013**, *51*, 3572−3582.

DOI: 10.1021/acsmacrolett.6b00349
ACS Macro Lett. 2016, 5, 790−795